AN APPLICATION OF THE NODE-BASED SMOOTHED FINITE ELEMENT METHOD FOR BUCKLING ANALYSIS OF LAMINATED COMPOSITE PLATES

by Tran Trung Dung[1] - Thai Hoang Chien[2]

ABSTRACT

An application of the node-based smoothed finite element method (NS-FEM) for buckling analyses of laminated composite plates using three-node triangular elements is exploited in this paper. A system stiffness matrix is calculated by using the strain smoothing technique over the smoothing domains associated with nodes of elements. In order to avoid the transverse shear locking and to improve the accuracy of the present formulation, the NS-FEM is incorporated with the discrete shear gap (DSG) method together with a stabilization technique to give a so-called node-based smoothed stabilized discrete shear gap method (NS-DSG). The numerical results derived from this method are compared with the solutions available in the literature to validate their reliability.

Keywords: Laminated composite platesm, node-based smoothed finite element method (NS-FEM), discrete shear gap (DSG) method.

1. Introduction

In recent years, laminated plates made of composite materials have been using intensively in many engineering application such as aerospace, marine and civil infrastructure. It is hence very essential to develop different numerical methods to model these structures flexibly and efficiently. In the aspect of theoretical formulation, these numerical methods are often based on three following popular plate theories: the classical laminated plate theory (CLPT), the first-order shear deformation laminated plate theory (FSDT), and higher-order shear deformation laminated plate theories (HSDT). In the aspects of numerical simulation, the low-order elements based on the first-oder shear deformation theory (FSDT) are preferred and still one of the most effective approaches due to their simplicity and computational efficiency. However, these FSDT-based elements often suffer from the shear locking phenomenon in the case of thin plates. To overcome it, various numerical techniques have been developed, such as the mixed formulation/ hybrid elements, the enhanced assumed strain (EAS) methods and the assumed natural strain (ANS) methods, e.g. book [1]. Recently, the discrete shear gap (DSG) method using triangular plate elements [2] was proposed by Bletzinger indicates that it can overcome shear-locking effectively.

In the other front of development of numerical methods, Liu and Nguyen-Thoi [3] integrated the strain smoothing technique [4] into the standard FEM to give a series of smoothed finite element methods (S-FEM). The advantage of the SFEM is that derivatives of the shape functions are not required, leading to lower computational cost because of the absence of an isoparametric mapping. SFEM has been developed four smoothed finite element methods (SFEMs) including a cell-based SFEM (CS-FEM) [6, 7], a node-based SFEM (NS-FEM) [8, 9], an edge-based SFEM (ES-FEM) [10, 11] and a face-based SFEM (FS-FEM) [12].

[1]*Faculty of Civil and Electrical Engineering, Ho Chi Minh City Open University, Vietnam*
[2]*Division of Computational Mechanics, Ton Duc Thang University, Vietnam*

Each of four new smoothing methods has different characters and advantages. Among of them, NS-FEM based on the idea of the node-based smoothed point interpolation method (NS-PIM) and the SFEM has been developed for 2D solid mechanics.

The aim of this paper is to describe a contribution to further development in this field, with the introduction and application of the node-based smoothed finite element method (NS-FEM) for buckling analysis of laminated composite plates using three-node triangular meshes. In order to eliminate shear locking, the NS-FEM is incorporated with the discrete shear gap (DSG) method to give a so-called node-based smoothed discrete shear gap method (NS-DSG). The numerical results derived from this method are compared with the solutions available in the literature to validate their accuracy.

2. Governing Equations

Consider a laminate consisting of n orthotropic layers with *a* total thickness h. Let Ω be a bounded region in R^2 occupied by the mid-plane of the plate and u_0, v_0, w_0 and $\beta = (\beta_x,\beta_y)$ denote the displacement components in the x, y, z directions and the rotations in the y-z and x-z planes, see Fig.1, respectively. The governing differential equations of the Mindlin–Reissner plate can be expressed by [13]:

$$u(x,y,z)=u^0(x,y)+z\beta_x(x,y)$$

$$v(x,y,z)=v^0(x,y)+z\beta_y(x,y)$$

$$w(x,y,z)=w^0(x,y)$$

The in-plane strain vector $\varepsilon_p=[\varepsilon_{xx}\ \varepsilon_{yy}\ \gamma_{xy}]^T$ and the transverse shear strain vector can be rewritten as

$$\varepsilon_p=\begin{bmatrix}\dfrac{\partial u_0}{\partial x}\\ \dfrac{\partial v_0}{\partial y}\\ \dfrac{\partial u_0}{\partial y}+\dfrac{\partial v_0}{\partial x}\end{bmatrix}+z\begin{bmatrix}\dfrac{\partial \beta_x}{\partial x}\\ \dfrac{\partial \beta_y}{\partial y}\\ \dfrac{\partial \beta_x}{\partial y}+\dfrac{\partial \beta_y}{\partial x}\end{bmatrix}=\varepsilon^m+z\varepsilon^b,\ \varepsilon^s=\begin{bmatrix}\varepsilon^s_{zx}\\ \varepsilon^s_{yz}\end{bmatrix}=\begin{bmatrix}\dfrac{\partial w}{\partial x}+\beta_x\\ \dfrac{\partial w}{\partial y}+\beta_y\end{bmatrix}$$

Figure 1: Geometry of a typical Mindlin-Reissner plate

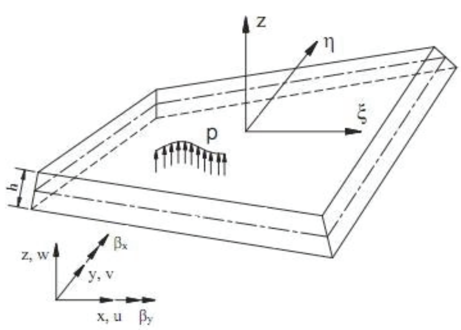

A weak form of the buckling model for Reissner/Mindlin composite plates can be briefly expressed respectively as:

$$\int_\Omega \delta\varepsilon_p^T\bar{\mathbf{D}}\varepsilon_p d\Omega+\int_\Omega(\delta\varepsilon^s)^T\mathbf{D}^s\varepsilon^s d\Omega+h\int_\Omega\begin{bmatrix}\nabla^T\delta u_0 & \nabla^T\delta v_0\end{bmatrix}\begin{bmatrix}\hat{\sigma}_0 & \mathbf{0}\\ \mathbf{0} & \hat{\sigma}_0\end{bmatrix}\begin{bmatrix}\nabla u_0\\ \nabla v_0\end{bmatrix}\mathrm{d}\Omega$$

$$+h\int_\Omega\nabla^T\delta w\hat{\sigma}_0\nabla w\mathrm{d}\Omega+\frac{h^3}{12}\int_\Omega\begin{bmatrix}\nabla^T\delta\beta_x & \nabla^T\delta\beta_y\end{bmatrix}\begin{bmatrix}\hat{\sigma}_0 & \mathbf{0}\\ \mathbf{0} & \hat{\sigma}_0\end{bmatrix}\begin{bmatrix}\nabla\beta_x\\ \nabla\beta_y\end{bmatrix}\mathrm{d}\Omega=0$$

(3)

where

$$\nabla^T = [\partial/\partial x \quad \partial/\partial y]^T,$$

$$\hat{\sigma}_0 = \begin{bmatrix} \sigma_x^0 & 0.5\tau_{xy}^0 \\ 0.5\tau_{xy}^0 & \sigma_y^0 \end{bmatrix}$$

are the gradient operator and in-plane pre-buckling stresses, respectively and

$$\bar{\mathbf{D}} = \begin{bmatrix} \mathbf{A} & \mathbf{B} \\ \mathbf{B} & \mathbf{D}^b \end{bmatrix} \qquad (4)$$

in which **A, B, D**^{b}**, D**^{s} matrices of extensional stiffness, bending-extensional coupling stiffness, bending stiffness and transverse shearing stiffness, respectively, defined as [13]

$$\left(\mathbf{A}_{ij}, \mathbf{B}_{ij}, \mathbf{D}_{ij}^b\right) = \int_{-h/2}^{h/2} \left(1, z, z^2\right) \bar{Q}_{ij} dz \qquad i, j = 1, 2, 6. \qquad (5)$$

$$\mathbf{D}_{ij}^s = k \int_{-h/2}^{h/2} \bar{Q}_{ij}^* dz \qquad i, j = 4, 5. \qquad (6)$$

where k denotes the transverse shear correction coefficient and $\bar{Q}_{ij}$ are the elastic constants.

Let's assume that the bounded domain Ω is discretized into *nel* finite elements such as $\Omega \approx \bigcup_{e=1}^{nel} \Omega^e$ and $\Omega^i \cap \Omega^j = \varnothing$, $i \neq j$. The finite element solution u^h of a displacement model for the Mindlin–Reissner plate is given by:

$$\mathbf{u}^h = \sum_{I=1}^{np} \begin{bmatrix} N_I(x) & 0 & 0 & 0 & 0 \\ 0 & N_I(x) & 0 & 0 & 0 \\ 0 & 0 & N_I(x) & 0 & 0 \\ 0 & 0 & 0 & N_I(x) & 0 \\ 0 & 0 & 0 & 0 & N_I(x) \end{bmatrix} \mathbf{d}_I \qquad (7)$$

where *np* is the total number of nodes, N_I, and $d_I = [u_I \quad v_I \quad w_I \quad \theta_{xI} \quad \theta_{yI}]^T$ are the shape function and the nodal degrees of freedom of u associated to node *I*, respectively. The membrane bending, shear strains and geometrical strains are expressed as:

$$\varepsilon_m = \sum_I \mathbf{B}_I^m \mathbf{d}_I, \quad \varepsilon^b = \sum_I \mathbf{B}_I^b \mathbf{d}_I, \quad \varepsilon^s = \sum_I \mathbf{B}_I^s \mathbf{d}_I, \quad \varepsilon^g = \sum_I \mathbf{B}_I^g \mathbf{d}_I \qquad (8)$$

where

$$\mathbf{B}_I^m = \begin{bmatrix} N_{I,x} & 0 & 0 & 0 & 0 \\ 0 & N_{I,y} & 0 & 0 & 0 \\ N_{I,y} & N_{I,x} & 0 & 0 & 0 \end{bmatrix}, \mathbf{B}_I^b = \begin{bmatrix} 0 & 0 & 0 & N_{I,x} & 0 \\ 0 & 0 & 0 & 0 & N_{I,y} \\ 0 & 0 & 0 & N_{I,y} & N_{I,x} \end{bmatrix}, \mathbf{B}_I^s = \begin{bmatrix} 0 & 0 & N_{I,x} & N_I & 0 \\ 0 & 0 & N_{I,y} & 0 & N_I \end{bmatrix} \qquad (9)$$

and

$$\mathbf{B}_I^g = \begin{bmatrix} N_{I,x} & N_{I,y} & 0 & 0 & 0 & 0 & 0 & 0 & 0 & 0 \\ 0 & 0 & N_{I,x} & N_{I,y} & 0 & 0 & 0 & 0 & 0 & 0 \\ 0 & 0 & 0 & 0 & N_{I,x} & N_{I,y} & 0 & 0 & 0 & 0 \\ 0 & 0 & 0 & 0 & 0 & 0 & N_{I,x} & N_{I,y} & 0 & 0 \\ 0 & 0 & 0 & 0 & 0 & 0 & 0 & 0 & N_{I,x} & N_{I,y} \end{bmatrix}^T \qquad (10)$$

The formulation of a Reissner–Mindlin plate can then be obtained for buckling analysis has the form respectively as

$$\left(\mathbf{K}-\lambda_{cr}\mathbf{K}_g\right)\mathbf{d}=0 \tag{11}$$

where the global stiffness matrix

$$\mathbf{K}=\int_\Omega(\mathbf{B}^m)^T\mathbf{A}\mathbf{B}^m d\Omega+\int_\Omega(\mathbf{B}^m)^T\mathbf{B}\mathbf{B}^b d\Omega+\int_\Omega(\mathbf{B}^b)^T\mathbf{B}\mathbf{B}^m d\Omega+\int_\Omega(\mathbf{B}^b)^T\mathbf{D}^b\mathbf{B}^b d\Omega+\int_\Omega(\mathbf{B}^s)^T\mathbf{D}^s\mathbf{B}^s d\Omega$$

(12)

and the global geometrical stiffness matrix is as follows

$$\mathbf{K}^g=\int_\Omega\left(\mathbf{B}^g\right)^T\boldsymbol{\tau}\,\mathbf{B}^g\mathrm{d}\Omega \tag{13}$$

in which

$$\boldsymbol{\tau}=\begin{bmatrix} h\hat{\sigma}_0 & 0 & 0 & 0 & 0\\ 0 & h\hat{\sigma}_0 & 0 & 0 & 0\\ 0 & 0 & h\hat{\sigma}_0 & 0 & 0\\ 0 & 0 & 0 & \frac{h^3}{12}\hat{\sigma}_0 & 0\\ 0 & 0 & 0 & 0 & \frac{h^3}{12}\hat{\sigma}_0 \end{bmatrix}$$

(14)

It is known that low-order triangular elements often occur shear locking in the limit of thin plates. Therefore, we introduce a simple triangular plate element NS-DSG3 [14] that combines the node-based smoothed finite element method (NS-FEM), a discrete shear gap (DSG) concept for shear-locking-free triangular Reissner-Mindlin plate-bending finite element (DSG3), and a stabilization technique proposed by Lyly *et al*. [15] aims to further improve the stability and the accuracy and helps to eliminate the shear locking for laminate composite plate.

3. The NS-FEM with Stabilized Discrete Shear Technique

In the NS-FEM, we do not use the compatible strain fields as in the standard FEM but use strains "smoothed" over local smoothing domains, and as a result the integration for the stiffness matrix is no longer based on elements, but based on these smoothing domains.

These local smoothing domains are constructed based on nodes of the elements such as $\Omega=\sum_{k=1}^{N_n}\Omega_k$ and $\Omega_i\cap\Omega_j=\varnothing$, $i\neq j$, in which N_n is the total number of nodes of all elements in the entire problem domain. For triangular elements, the smoothing domain Ω_k associated with the node k is created by connecting sequentially the mid-edge-point to centroids of the surrounding triangles of the node as shown in Fig.2. Introducing smoothing strains over the smoothing domain Ω_k, one writes

$$\tilde{\varepsilon}_k^m=\int_{\Omega_k}\varepsilon^m(\mathbf{x})\Phi(\mathbf{x})\mathrm{d}\Omega,\ \tilde{\varepsilon}_k^b=\int_{\Omega_k}\varepsilon^b(\mathbf{x})\Phi(\mathbf{x})\mathrm{d}\Omega,\ \tilde{\varepsilon}_k^s=\int_{\Omega_k}\varepsilon^s(\mathbf{x})\Phi(\mathbf{x})\mathrm{d}\Omega,\ \tilde{\varepsilon}_k^g=\int_{\Omega_k}\varepsilon^g(\mathbf{x})\Phi(\mathbf{x})\mathrm{d}\Omega$$

(15)

where Φ(x) is a given smoothing function that satisfies at least unity property

$$\int_{\Omega_k}\Phi(\mathbf{x})\mathrm{d}\Omega=1 \tag{16}$$

and in this work Φ(x) is assumed to be a step function given by

$$\Phi(\mathbf{x})=\begin{cases}1/A_k & \mathbf{x}\in\Omega_k\\ 0 & \mathbf{x}\notin\Omega_k\end{cases} \tag{17}$$

Where $A_k=\int_{\Omega_k}\mathrm{d}\Omega$ is the area of the smoothing domain Ω_k and computed by $A_k=\int_{\Omega_k}\mathrm{d}\Omega=\frac{1}{3}\sum_{i=1}^{N_k^e}A_i^e$ where N_k^e is the number of elements connected to the node k and A_i^e is the area of the i^{th} element around the node k. Substituting Eqs. (8) and (17) into (15), the smoothed strains at node k can be expressed in the following form:

$$\tilde{\varepsilon}_k^m = \frac{1}{A_k}\int_{\Omega_k} \varepsilon^m(\mathbf{x})\mathrm{d}\Omega = \sum_{I=1}^{N_k^n} \tilde{\mathbf{B}}_I^m(x_k)\mathbf{d}_I,\ \tilde{\varepsilon}_k^b = \sum_{I=1}^{N_k^n} \tilde{\mathbf{B}}_I^b(x_k)\mathbf{d}_I,$$
$$\tilde{\varepsilon}_k^s = \sum_{I=1}^{N_k^n} \tilde{\mathbf{B}}_I^s(x_k)\mathbf{d}_I,\ \tilde{\varepsilon}_k^g = \sum_{I=1}^{N_k^n} \tilde{\mathbf{B}}_I^g(x_k)\mathbf{d}_I \tag{18}$$

where N_k^e is the total number of nodes belonging to elements directly connected to node k. $\tilde{\mathbf{B}}_I^m$ and $\tilde{\mathbf{B}}_I^b$ are the smoothed gradient matrices through the smoothing domain $\mathbf{\Omega}_k^s$ and are given by

$$\tilde{\mathbf{B}}_I^m = \frac{1}{A_k}\sum_{i=1}^{N_k^e}\frac{1}{3}A_i^e\mathbf{B}_i^m,\ \tilde{\mathbf{B}}_I^b = \frac{1}{A_k}\sum_{i=1}^{N_k^e}\frac{1}{3}A_i^e\mathbf{B}_i^b,\ \tilde{\mathbf{B}}_I^s = \frac{1}{A_k}\sum_{i=1}^{N_k^e}\frac{1}{3}A_i^e\mathbf{B}_i^{sDSG3},\ \tilde{\mathbf{B}}_I^g = \frac{1}{A_k}\sum_{i=1}^{N_k^e}\frac{1}{3}A_i^e\mathbf{B}_i^g \tag{19}$$

where $\mathbf{B}_i^m$ and $\mathbf{B}_i^b$ are obtained from the three-node standard finite element

$$\mathbf{B}_i^m = \frac{1}{2A^e}\begin{bmatrix} b-c & 0 & 0 & 0 & 0 & c & 0 & 0 & 0 & 0 & -b & 0 & 0 & 0 & 0 \\ 0 & d-a & 0 & 0 & 0 & 0 & -d & 0 & 0 & 0 & 0 & a & 0 & 0 & 0 \\ d-a & b-c & 0 & 0 & 0 & -d & c & 0 & 0 & 0 & a & -b & 0 & 0 & 0 \end{bmatrix} \tag{20}$$

$$\mathbf{B}_i^b = \frac{1}{2A^e}\begin{bmatrix} 0 & 0 & 0 & b-c & 0 & 0 & 0 & 0 & c & 0 & 0 & 0 & 0 & -b & 0 \\ 0 & 0 & 0 & 0 & d-a & 0 & 0 & 0 & 0 & -d & 0 & 0 & 0 & 0 & a \\ 0 & 0 & 0 & d-a & b-c & 0 & 0 & 0 & -d & c & 0 & 0 & 0 & a & -b \end{bmatrix} \tag{21}$$

while $\mathbf{B}_i^{sDSG}$ is derived from the discrete shear gap technique [2]

$$\mathbf{B}_i^{sDSG} = \frac{1}{2A^e}\begin{bmatrix} 0 & 0 & b-c & A^e & 0 & 0 & 0 & c & \frac{ac}{2} & \frac{bc}{2} & 0 & 0 & -b & -\frac{bd}{2} & -\frac{bc}{2} \\ 0 & 0 & d-a & 0 & A^e & 0 & 0 & -d & -\frac{ad}{2} & -\frac{bd}{2} & 0 & 0 & a & \frac{ad}{2} & \frac{ac}{2} \end{bmatrix} \tag{22}$$

and $\mathbf{B}_i^g$ has the following form

$$\mathbf{B}_i^g = \frac{1}{2A^e}\begin{bmatrix} b-c & 0 & 0 & 0 & 0 & c & 0 & 0 & 0 & 0 & -b & 0 & 0 & 0 & 0 \\ d-a & 0 & 0 & 0 & 0 & -d & 0 & 0 & 0 & 0 & a & 0 & 0 & 0 & 0 \\ 0 & b-c & 0 & 0 & 0 & 0 & c & 0 & 0 & 0 & 0 & -b & 0 & 0 & 0 \\ 0 & d-a & 0 & 0 & 0 & 0 & -d & 0 & 0 & 0 & 0 & a & 0 & 0 & 0 \\ 0 & 0 & b-c & 0 & 0 & 0 & 0 & c & 0 & 0 & 0 & 0 & -b & 0 & 0 \\ 0 & 0 & d-a & 0 & 0 & 0 & 0 & -d & 0 & 0 & 0 & 0 & a & 0 & 0 \\ 0 & 0 & 0 & b-c & 0 & 0 & 0 & 0 & c & 0 & 0 & 0 & 0 & -b & 0 \\ 0 & 0 & 0 & d-a & 0 & 0 & 0 & 0 & -d & 0 & 0 & 0 & 0 & a & 0 \\ 0 & 0 & 0 & 0 & b-c & 0 & 0 & 0 & 0 & c & 0 & 0 & 0 & 0 & -b \\ 0 & 0 & 0 & 0 & d-a & 0 & 0 & 0 & 0 & -d & 0 & 0 & 0 & 0 & a \end{bmatrix} \tag{23}$$

with $a = x_2 - x_1$, $b = y_2 - y_1$, $c = y_3 - y_1$, $d = x_3 - x_1$, $((x_i, y_i)$, i=1,2,3 are three vertical coordinates of element), see Fig.3 and A^e is the area of triangular element.

Figure 2: Three-node triangular mesh and smoothing domains

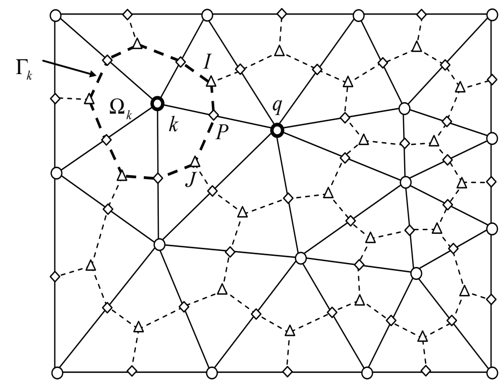

Figure 3: Three -node triangular element

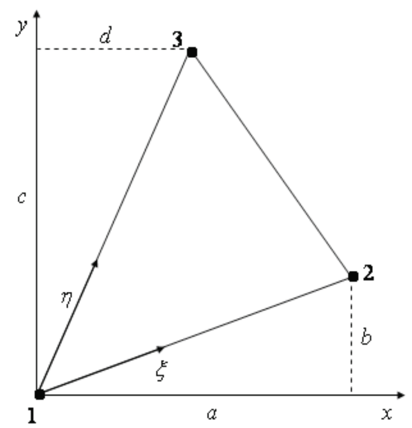

Therefore the global stiffness and geometrical stiffness matrices of the NS-DSG3 element are assembled by

$$\tilde{\mathbf{K}} = \sum_{k=1}^{N_n} \tilde{\mathbf{K}}_k \, , \, \tilde{\mathbf{K}}^g = \sum_{k=1}^{N_n} \tilde{\mathbf{K}}_k^g \tag{24}$$

where the nodal stiffness matrix $\tilde{\mathbf{K}}_k$ of the NS-DSG3 element is given by

$$\tilde{\mathbf{K}}_k = (\tilde{\mathbf{B}}^m)^T \mathbf{A} \tilde{\mathbf{B}}^m A_k + (\tilde{\mathbf{B}}^m)^T \mathbf{B} \tilde{\mathbf{B}}^b A_k + (\tilde{\mathbf{B}}^b)^T \mathbf{B} \tilde{\mathbf{B}}^m A_k + (\tilde{\mathbf{B}}^b)^T \mathbf{D}^b \tilde{\mathbf{B}}^b A_k + (\tilde{\mathbf{B}}^s)^T \mathbf{D}^s \tilde{\mathbf{B}}^s A_k$$

$$\tilde{\mathbf{K}}_k^g = \int_{\Omega_k} \tilde{\mathbf{B}}^{gT} \boldsymbol{\tau} \, \tilde{\mathbf{B}}^g \mathrm{d}\Omega = \tilde{\mathbf{B}}^{gT} \boldsymbol{\tau} \, \tilde{\mathbf{B}}^g A_k \tag{25}$$

It was mentioned that a stabilization technique [15] needs to be added to the DSG3 element to improve significantly approximate solutions and to avoid shear force oscillations presenting in the case of triangles. For this remedy, the nodal stiffness matrix of the NS-DSG3 element can be also modified as

$$\tilde{\mathbf{K}}_k = (\tilde{\mathbf{B}}^m)^T \mathbf{A} \tilde{\mathbf{B}}^m A_k + (\tilde{\mathbf{B}}^m)^T \mathbf{B} \tilde{\mathbf{B}}^b A_k + (\tilde{\mathbf{B}}^b)^T \mathbf{B} \tilde{\mathbf{B}}^m A_k + (\tilde{\mathbf{B}}^b)^T \mathbf{D}^b \tilde{\mathbf{B}}^b A_k + (\tilde{\mathbf{B}}^s)^T \overline{\mathbf{D}}^s \tilde{\mathbf{B}}^s A_k \tag{26}$$

in which

$$\bar{\mathbf{D}}^s = \frac{h^2}{h^2 + \alpha h_k^2}\mathbf{D}^s \qquad (27)$$

where $h_k = \sqrt{A_k}$ is the average length of the smoothing domain Ω_k and $\alpha \in [0.05 \div 0.15]$ is a arbitrary positive constant. It is fixed α = 0.05.

4. Numerical Results

Some numerical examples are presented to compare with the other solutions in the analysis buckling of laminated plates. In all the following examples, all layers of the laminated plate are assumed to be of the same thickness, mass density, and made of the same linearly elastic composite material. The material properties are assumed: $E_1/E_2 = 40$; $G_{12} = G_{13} = 0.6E_2$, $G_{23} = 0.5E_2$; $\nu_{12} = 0.25$, $\rho = 1$.

Unless otherwise stated, the shear correction factor $k = \pi^2/12$ is used for all computations and the buckling load factor is defined as $\bar{\lambda} = \lambda_{cr} a^2 / (E_2 h^3)$. Where a, h and λ_{cr} are the edge length, thickness of the composite plate and the critical buckling load, respectively.

4.1. Square Plate under Uniaxial Compression

Let's first consider a simply supported four-layer cross-ply [$0^0/90^0/90^0/0^0$] square laminated plate with the length a and the thickness h subjected to uniaxial compression as shown in Fig.4a. In this problem, we study the effect and accuracy of NS-DSG3 for various modulus ratios. The length-to-thickness ratio of the plate a/h is taken to be 10. Table 1 presents the convergence of the normalized critical buckling load of a simply supported four-layer cross-ply [$0^0/90^0/90^0/0^0$] square laminated with the various modulus ratios. The results of the present method are compared with the 3D elasticity solution [16], RPIM solution based on FSDT [17] and FEM solution based on HSDT [18, 19]. It can be seen that the present results agree well with those solutions and the normalized critical buckling loads increase with increasing of the E_1/E_2 modulus ratios. Comparing with the reference solution obtained in 3D elasticity, it is observed that the NS-DSG3 solution is quite insensitive to the variation of modulus ratios as seen in Fig.5.

Next, the effect of the length-to-thickness ratio a/h on the uniaxial compression load is also considered for two and four layer simply supported cross-ply square plates. The normalized critical buckling load of the present method is compared with the solutions in Nguyen *et al*. [20], Chakrabarti and Sheikh [21] and Reddy and Phan [22]. Table 2 shows the normalized critical buckling load of two and four layer simply supported plate. It is seen that the present result gives a good agreement with available solutions and the normalized critical buckling load decreases with the decreasing length-to-thickness ratio a/h.

Table 1: A normalized critical buckling loads of simply supported cross-ply [$0^0/90^0/90^0/0^0$] square plate with various E_1/E_2 ratios.

Methods	Mesh	E_1/E_2				
		3	10	20	30	40
	8 x 8	5.6227	10.3599	15.9163	20.4334	24.2024
NS-DSG3	12 x 12	5.4528	10.0596	15.4829	19.9084	23.6136
	16 x 16	5.3939	9.9552	15.3313	19.7238	23.4055

Noor [16]	5.294	9.761	15.019	19.304	22.88
RPIM [17]	5.401	9.985	15.374	19.537	23.154
HSDPT [18]	5.114	9.774	15.298	19.957	23.34
HSDT [19]	5.442	10.026	15.418	19.813	23.489

Table 2: A normalized critical buckling loads of simply supported cross-ply square plate with various *a/h* ratios.

Number layer	Methods	*a/h*			
		10	**20**	**50**	**100**
$[0^0/90^0]$	MISQ20 [20]	11.169	12.52	12.967	13.033
	FSDT (Chakrabarti *et al.*) [21]	11.349	12.51	12.879	12.934
	FSDT (Reddy and Phan) [22]	11.353	12.515	12.884	12.939
	HSDT (Reddy and Phan) [22]	11.563	12.577	12.895	12.942
	NS-DSG3 (16 x 16)	11.2445	12.6172	13.0723	13.1433
$[0^0/90^0/90^0/0^0]$	MISQ20 [20]	23.236	31.747	35.561	36.19
	FSDT (Chakrabarti *et al.*) [21]	23.409	31.625	35.254	35.851
	FSDT (Reddy and Phan) [22]	23.471	31.707	35.356	35.955
	HSDT (Reddy and Phan) [22]	23.349	31.637	35.419	35.971
	NS-DSG3 (16 x 16)	23.4055	32.0186	35.8846	36.5222

Figure 4: Geometry of laminated composite plates under axial and biaxial compression

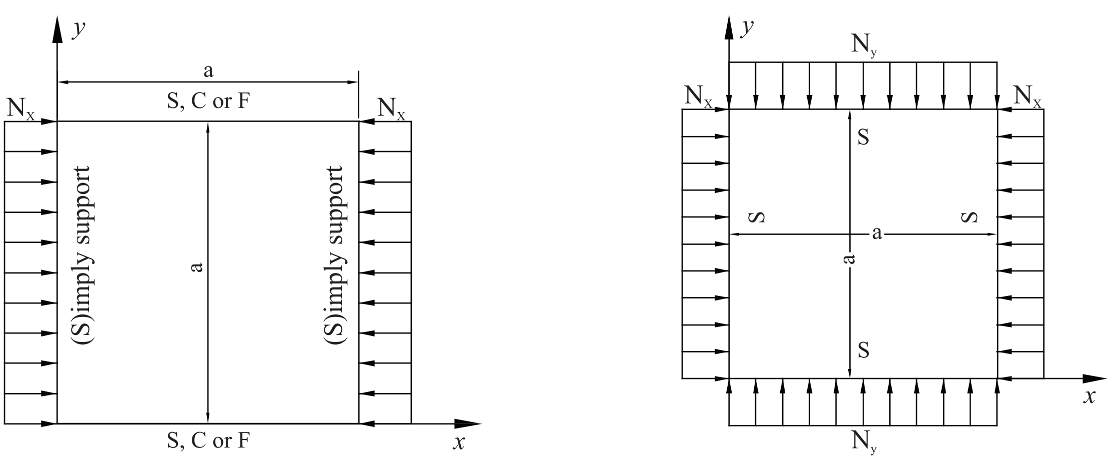

(a) (b)

Figure 5: Effect of modulus ratios on the accuracy of critical buckling loads

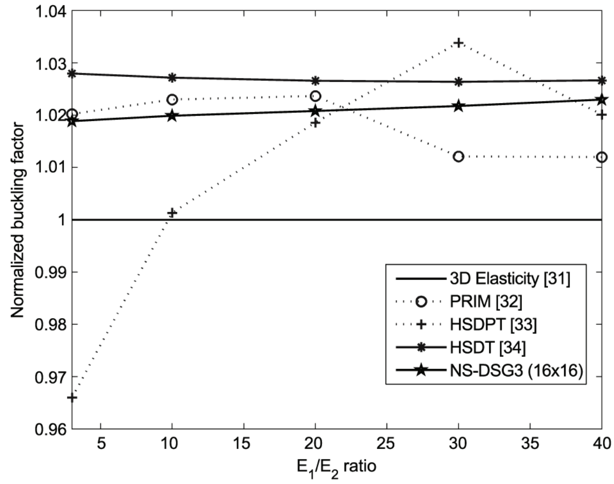

We also consider the influence of the mixed boundary conditions of two layers cross-ply square plate with length-to-thickness ratios *a/h* = 10 and modulus ratios E_1/E_2 = 40. Table 3 shows the normalized critical buckling load factors with various boundary condition SSSS, SSFF, SSCC, SSFC and SSFS plates. It can be seen that the NS-DSG3 works well compared with several other methods such as MISQ20 [20], the moving least square differential quadrature method (MLSDQ) [23], the meshless method using FSDT (RKPM) [24] and FEM [25]. The buckling mode shapes are also displayed in Fig.6.

Table 3: A normalized critical buckling loads of cross-ply [$0^0/90^0$] with various mixed boundaries (E_1/E_2 = 40; *a/h* = 10)

Methods	Boundary conditions				
	SSSS	SSFF	SSCC	SSSC	SSFC
MISQ20 [20]	11.291	4.86	20.082	16.47	6.14
MLSDQ [23]	11.301	4.823	19.871	-	-
RKPM (Wang *et al.*, 2002)[24]	11.582	4.996	20.624	16.872	6.333
FSDT (Reddy and Khdeir) [25]	11.353	4.851	20.067	16.437	6.166
HSDT (Reddy and Khdeir) [25]	11.562	4.94	21.464	17.133	6.274
NS-DSG3 (8 x 8)	11.6878	4.8319	20.9502	16.5550	6.2592
NS-DSG3 (12 x 12)	11.3587	4.8144	20.0564	16.2743	6.1721
NS-DSG3 (16 x 16)	11.2445	4.8058	19.7551	16.1798	6.1377

Figure 6: Buckling mode shapes of [0/90] laminated plate with various boundary conditions

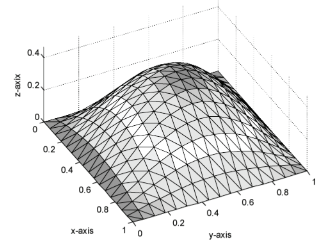

(a) SSSS

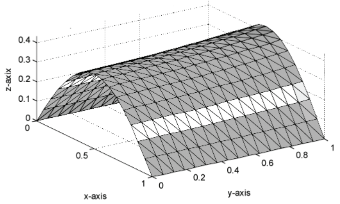

(b) SSFF

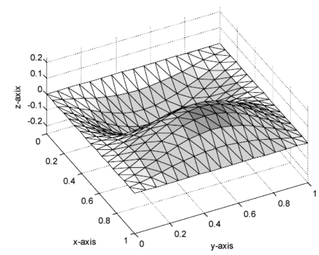

(c) SSCC

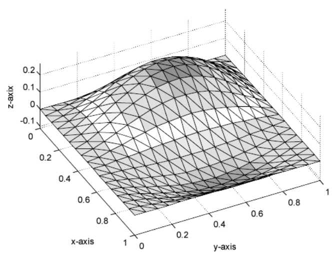

(d) SSSC

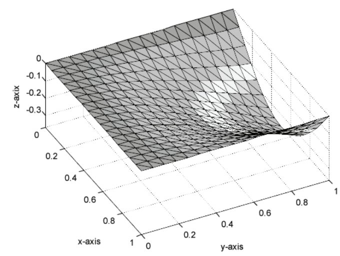

(e) SSFC

4.2. Square Plate under Biaxial Compression

The final example considers the 3-layer symmetric cross-ply [$0^0/90^0/0^0$] simply supported plate subjected to the bi-axial buckling load as shown in Fig.4b. The span-to-thickness ratio *a/h* is taken to be 10 and the modulus ratios $E_1/E_2 = 40$. The effect of modulus ratio E_1/E_2 on the critical bi-axial buckling load is studied in this section. Table 4 shows the normalized critical buckling loads. It can be seen that the present element provides reasonable results compared with other published methods.

Table 4: Biaxial buckling of simply supported cross-ply [$0^0/90^0/0^0$] square plate with various modulus ratio.

Methods	E_1/E_2			
	10	**20**	**30**	**40**
HSDT (Khdeir and Librescu) [19]	4.963	7.516	9.056	10.259
FSDT (Fares and Zenkour) [26]	4.963	7.588	8.575	10.202
MISQ20 [20]	4.939	7.488	9.016	10.252
NS-DSG3 (8 x 8)	5.1316	7.7686	9.7658	11.1039
NS-DSG3 (12 x 12)	4.9820	7.5540	9.1805	10.4296
NS-DSG3 (16 x 16)	4.9299	7.4788	8.9728	10.2010

5. Conclusion

In this paper, an application of the node-based smoothed finite element method with discrete shear gap technique has been presented for buckling analyses of laminated composite plates based on FSDT to give a so-call node-based smoothed discrete shear gap method (NS-DSG). The results of the NS-DSG3 element showed that it can outperform several reference

3-noded triangular elements and can provide more reliable results compared to other published methods. The present method is thus very promising to provide a simple and effective tool for buckling analysis of composite plate structures.

REFERENCES

1. Zienkiewicz, O.C., Taylor, R.L.: The finite element method (5th edn.). Butterworth Heinemann, Oxford (2000)
2. Bletzinger, K.U., Bischoff, M., Ramm, E.: A unified approach for shear-locking free triangular and rectangular shell finite elements. Computers and Structures. **75**, 321–334 (2000).
3. Liu, G.R., Nguyen-Thoi, T.: Smoothed Finite Element Methods. CRC Press, Taylor and Francis Group, NewYork (2010)
4. Chen, J.S., Wu, C.T., Yoon, S., You, Y.: A stabilized conforming nodal integration for galerkin mesh-free methods. International Journal for Numerical Methods in Engineering. **50**, 435-466 (2001)
5. Liu, G.R.: Meshfree methods: Moving beyond the finite element method. CRC Press: Boca Raton, Florida (2009)
6. Liu, G.R., Dai, K.Y., Nguyen-Thoi, T.: A smoothed finite element for mechanics problems. Computational Mechanics. **39**, 859-877 (2007)
7. Liu, G.R., Nguyen-Thoi, T., Dai, K.Y., Lam, K.Y.: Theoretical aspects of the smoothed finite element method (SFEM). International Journal for Numerical Methods in Engineering. **71**, 902-930 (2007)
8. Liu, G.R., Nguyen-Thoi, T., Nguyen-Xuan, H., Lam, K.Y.: A node-based smoothed finite element method (NS-FEM) for upper bound solutions to solid mechanics problems. Computers and Structures. **87**, 14-26 (2009).
9. Nguyen-Xuan, H., Rabczuk, T., Nguyen-Thanh, N., Nguyen-Thoi, T., Bordas, S.: A node-based smoothed finite element method with stabilized discrete shear gap technique for analysis of Reissner-Mindlin plates, Comput. Mech., **46**, 679–701 (2010)
10. Liu, G.R., Nguyen-Thoi, T., Lam, K.Y.: An edge-based smoothed finite element method (ES-FEM) for static and dynamic problems of solid mechanics. Journal of Sound and Vibration. **320**, 1100 – 1130 (2009).
11. Nguyen-Xuan, H., Liu, G.R., Thai-Hoang, C., Nguyen-Thoi, T.: An edge-based smoothed finite element method with stabilized discrete shear gap technique for analysis of Reissner-Mindlin plates. Computer Methods in Applied Mechanics and Engineering. **199**, 471–489 (2009)
12. Nguyen-Thoi, T., Liu, G.R., Lam, K.Y.: A Face-based Smoothed Finite Element Method (FS-FEM) for 3D linear and nonlinear solid mechanics problems using 4-node tetrahedral. Int J Numer Methods Eng. **78**, 324–353 (2009)
13. Reddy, J.N.: Mechanics of laminated composite plates and shells: theory and analysis. second edn. London: CRC Press (2004)
14. Nguyen-Xuan, H., Rabczuk, T., Nguyen-Thanh, N., Nguyen-Thoi, T., Bordas, S.: A node-based smoothed finite element method with stabilized discrete shear gap technique for analysis of Reissner–Mindlin plates, Comput Mech. **46**, 679–701 (2010)

15. Lyly, M., Stenberg, R., Vihinen, T.: A stable bilinear element for the Reissner–Mindlin plate model. Computer Methods in Applied Mechanics and Engineering. **110**, 343–357 (1993)
16. Noor, A.K., Mathers, M.D.: Shear-flexible finite element method of laminated composite plate,Technical report, NASA (1975)
17. Liu, L., Chua, L.P., Ghista, D.N.: Mesh-free radial basis function method for static, free vibration and buckling analysis of shear deformable composite laminates. Composite Structures. **78** 58–69 (2007)
18. Phan, N.D., Reddy, J.N.: Analysis of laminated composite plates using a higher-order shear deformation theory. International Journal for Numerical Methods in Engineering. **21**, 2201–2219 (1985)
19. Khdeir, A.A., Librescu, L.: Analysis of symmetric cross-ply elastic plates using a higher-order theory. Part ii: buckling and free vibration. Composite Structures. **9**, 259–277 (1988)
20. Nguyen-Van, H.: Development and application of assumed strain smoothing finite element technique for composite plate/shell structures, Faculty of Engineering and Surveying – University of Southern Queensland, Ph.D. Thesis (2009)
21. Chakrabarti, A., Sheikh, A.H.: Buckling of laminated composite plates by a new element based on higher order shear deformation theory. Mechanics of Composite Materials and Structures. **10** (4), 303–317 (2003)
22. Reddy, J.N., Phan, P.H.: Stability and vibration of isotropic, orthotropic and laminated plates according to a higher order shear deformation theory. Journal of Sound and Vibration. **89**, 157–170 (1985)
23. Huang, Y.Q., Li, Q.S.: Bending and buckling analysis of antisymmetric laminates using the moving least square differential quadrature method. Computer Methods in Applied Mechanics and Engineering. **193** (33–35) (2004) 3471–3492.
24. Wang, J., Liew, K.M., Tan, M.J., Rajendran, S.. Analysis of rectangular laminated composite plates via fsdt meshless method. International Journal of Mechanical Sciences. **44** (7), 1275–1293 (2002)
25. Reddy, J.N., Khdeir, A.A.: Buckling and vibration of laminated composite plates using various plate theories. AIAA Journal. **27** (12), 1808–1817 (1989)
26. Fares, M.E., Zenkour, A.M.: Buckling and free vibration of non-homogeneous composite cross-ply laminated plates with various plate theories. Composite Structures **44**, 279–287 (1999)